JOURNAL OF MATERIALS SCIENCE 18 (1983) 903–918

Application of the plane simple shear test for determination of the plastic behaviour of solid polymers at large strains

CHRISTIAN G'SELL, SERGE BONI
Laboratoire de Physique du Solide (LA au CNRS No. 155) ENSMIM, Parc de Saurupt, 54042 Nancy, France

SURESH SHRIVASTAVA
Department of Civil Engineering and Applied Mechanics, McGill University, 817 Sherbrooke Street West, Montreal, Quebec, Canada

A simple shear test apparatus was designed and used in experiments for determining the plastic behaviour of various amorphous and semicrystalline polymers at large shear strains. The geometry and dimensions of the specimens were determined after a critical evaluation of the test conditions, so as to avoid plastic buckling of the specimens, and to minimize undesirable stresses at the specimen ends. Using the present technique, it was possible to conduct tests at room temperature up to strains of 200% for polymethyl methacrylate (PMMA) and 1000% for polyethylene, without extensive crazing. Optimum precision and homogeneity of strains within the samples could be achieved because of firm guiding of the gripped specimen heads during the tests. A systematic study of the influence of shear strain rate and temperature on the plastic behaviour was made particularly for the polyethylene samples. The kinematics of large deformation simple shear is discussed and relations between the stress and the finite-strain tensors is presented, with particular attention being paid to the development of normal stresses. The problem of end effects is also investigated. Finally, it is shown that the strain hardening of polyethylene under simple shear is much smaller than under uniaxial tension. A possible interpretation of this behaviour is proposed in terms of the uniqueness versus multiplicity of slip systems.

1. Introduction

The plastic behaviour of solid polymers at large strains has been investigated to a small extent, and only more recently, than the yield behaviour of solid polymers. While many authors have investigated the change in the yielding conditions with the type of loading in amorphous and semicrystalline polymers, only little is known about the influence of deformation geometry on the determination of constitutive equations of plastic flow. This is because, until recently, the mechanical applications of polymers mostly required knowledge of their viscoelastic properties. However, the solution of problems now encountered in the development of forming techniques, involving multiaxial plastic deformation (thermoforming, biaxial film drawing, solid extrusion or forging, etc.) requires a precise determination of the plastic properties of these materials for a wide range of temperature, strain rate and deformation geometry.

The first efforts directed to this end were concerned with the tensile testing of thermoplastics at large strains. Tensile stress–strain relations were obtained at fixed strain rates and temperatures, e.g. [1–4], and computer methods were developed to deduce from these relations the evolution of the deformation of polymer rods

0022–2461/83/030903–16$04.42/0

or plates subjected to an arbitrary elongation sequence [5, 6].

Another elementary mode of deformation, which may be used for the determination of plastic properties, is that of shearing. It has been shown several times [7, 8] that it constitutes the basic process in the development of bands in the plastic deformation of glassy polymers. In order to obtain a shear stress against shear strain relationship, several authors have applied the conventional torsion test to polymers [9–11]. However, the main limitation of this test stems from the fact that the stress and strain fields are nonhomogeneous. Hence, a precise transformation of the torque-twist experimental data into true stress–true strain curves is not possible unless rough approximations are used. With the view of testing polymers under conditions as close as possible to pure shear a plane-strain compression technique [12] was also developed and applied to acrylics. Unfortunately, the complexity of this test and the friction forces at the compression tool surface impose serious limitations on its application to large strain testing. Finally, for determining particular characteristics (like the shear resistance of fibre reinforced composites), a short beam shear test in three-point bending [13] has been standardized; however, again due to the nonhomogeneous and complex state of deformation that is produced in the specimens, it cannot be applied to large strain testing.

In contrast to the preceding types of tests, it may be noted that the plane simple shear method of testing is better suited to the determination of intrinsic material properties. In principle, it does not involve the strain inhomogeneities that are inherent in the torsion and bending tests, and it requires imposition of simpler boundary conditions than those used in the plane-strain compression test. Simple shear tests were initially applied to oriented thin polymer films, for the purpose of determining the shear yield stress as a function of the angle between the shearing direction and the orientation axis [14–16]. They have also been used in a fundamental study of the yield behaviour of glassy polymer films [17, 18]. A review of these papers indicates that the main problems encountered in the tests were associated with the insufficient thickness of the specimens, which resulted in plastic buckling and unwanted deformation in the grips.

The aim of the present paper is to show that the plane simple shear test can be used with confidence to determine the plastic behaviour of solid polymers, provided that the geometry of the specimens and the mechanical features of the test apparatus are correctly chosen. A new type of testing method has been proposed and used. The results of tests on various amorphous and semicrystalline thermoplastic polymers are presented. In the particular case of high density polyethylene, the plastic behaviour in simple shear will be compared with that in uniaxial tension.

2. Experimental procedures

2.1. Characteristics of the simple shear test

The simple shear deformation of a parallelepiped solid can be basically defined, as illustrated in Fig. 1, by the homogeneous relative glide of parallel planes normal to the Ox_2 axis along the shear direction Ox_1. The amount of shear is conventionally expressed (Dieter [19]) by the ratio $\gamma = x/h$, where x is the relative displacement of the opposite faces of the parallelepiped and h is the sheared width of the sample. In order to impose a constant shear rate $\dot{\gamma} = d\gamma/dt$, the opposite faces are displaced at a constant velocity $\dot{x} = h\dot{\gamma}$. The conventional shear stress will be defined by $\tau = F/(Le)$, where F is the shearing force applied to the faces normal to Ox_2 and L is the length of the initial parallelepiped and e its thickness. The simple shear behaviour of a given

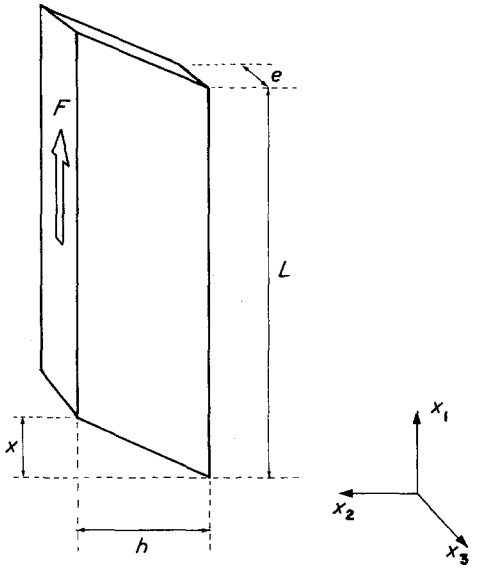

Figure 1 Definition of the reference axes and dimensions of a parallelepipedic piece of material deformed in simple shear.

material can be expressed as a shear stress versus shear relation, $\tau(\gamma)$, at a fixed values of shear rate $\dot{\gamma}$ and temperature T.

2.2. Geometry and dimensions of the samples

The experimental application of a simple shear test requires a judicious choice of the specimen size. Otherwise, as will be seen, the effective distribution of stresses and strains within the material is far from a homogeneous one, and the $\tau(\gamma)$ curves obtained from the test may not represent the shear stress–shear strain behaviour accurately.

The first problem in the testing of specimens in shear is their possible buckling if the thickness e is not large enough. This difficulty was encountered by all the authors who applied the shear test to thin polymer films [14–18]. It has been shown in another paper by Boni *et al.* [20] that the oblique folds exhibited by the sheared films are due to the action of compressive stresses which are developed in simple shear along a direction inclined to the shearing direction. In the case of infinitesimal shear strain, it is known, for example Hearn [21], that a principal compressive stress $\sigma_2 = -\tau$ appears along the direction bisecting the $-Ox_1$ and Ox_2 axis (Fig. 2a). As will be seen in the discussion, this simple situation is somewhat perturbed in the case of large strains, but essentially the oblique compressive stresses continue to exist. The buckling of an elastic plate stressed in simple shear has been analysed in the literature (see for example, Southwell [22], Bleich and Bleich [23], and Timoshenko and Gere [24]). According to Bleich and Bleich [23], the plastic buckling normally occurs when the applied shear stress approaches the critical value $\tau_c = k\pi^2 D\eta/h^2 e$ where $D = Ee^3/12(1-\nu^2)$ is the flexural rigidity of the plate, E is Young's modulus, ν is Poisson's ratio, k is a coefficient which depends upon the aspect ratio, L/h, of the plate and the boundary conditions (e.g. free or fixed edges) and η is a plastic softening factor approximately equal to $(\theta/E)^{1/2}$, where θ is the strain hardening rate (e.g. the tangent modulus) at τ_c. For $L/h > 4$, and for edges of the plate rigidly gripped, a conservative value of the coefficient k is equal to about 9. Using this value, in the condition of no buckling, $\tau_c > \tau_{max}$, we get the first dimensional relation:

$$\left(\frac{e}{h}\right)^2 > \frac{12\tau_{max}(1-\nu^2)}{9\pi^2 E\eta} \qquad (1)$$

Taking as reasonable values $\tau_{max} \approx 200$ MPa, $E \approx 1000$ MPa, $\eta \approx 0.12$ and $\nu = 0.35$, it is found that the thickness to width ratio of the specimens must be larger than about 0.44 to ensure that buckling will not occur during the shear test.

A second limitation on the dimensions arises from the necessity of minimizing the unwanted normal stresses due to the grip constraints. As shown in Fig. 2b, the couple of shearing forces applied on the two faces of the specimen at a distance h apart gives rise to a rotational moment Fh, which must be counterbalanced by the forces exerted on the sample by the grips. These reaction forces give rise to stresses which are perpendicular to the shearing direction. Obviously, these normal stresses vary from compression to tension along the specimen faces and across the width. If one considers, as a first approximation, that this variation is linear, then by equating the two moments, it is found that

$$Fh = \tfrac{4}{3}|\bar{\sigma}_N| eL^2 \qquad (2)$$

where $|\bar{\sigma}_N|$ is the mean absolute value of these normal stresses within the sample. A reasonable minimization of this effect consists in ensuring that $|\bar{\sigma}_N|$ is less than or equal to 5% of the applied shear stress $\tau = F/(Le)$. This leads to the second dimensional relation:

$$\frac{L}{h} > 15 \qquad (3)$$

It will be shown later in the discussion, that for a particular case, the linear approximation taken

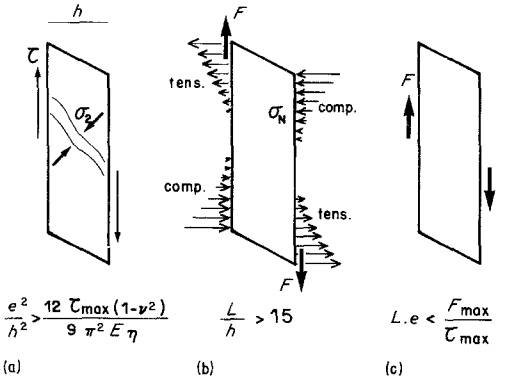

Figure 2 Diagrams illustrating the three geometrical limitations imposed in a simple shear test: (a) no buckling condition, (b) normal stress minimization, and (c) maximum capacity of the testing machine.

above is a rather pessimistic one and that the real distribution tends to significantly decrease the mean value $|\bar{\sigma}_N|$.

Lastly, one has to take into account the maximum loading capacity, F_{max}, of the machine which is used to apply the shearing forces. If τ_{max} is the maximum shear stress of the tested material at rupture, we get the third dimensional relation (Fig. 2c)

$$Le < \frac{F_{max}}{\tau_{max}} \quad (4)$$

In the present case, with a hydraulic actuator whose capacity is 50 kN, and considering the maximum shear stress for polymers to be lower than 250 MPa, Equation 4 imposes the limitation $Le < 200\,mm^2$. Combining this result with Equations 1 and 3, the standard specimen dimensions were selected as $L = 60$ mm, $h = 4$ mm and $e = 3$ mm.

As shown by Boni *et al.* [20] in an earlier publication on shear tests on thin films, the films suffered from unwanted deformations of the material within the gripped portion of the specimens. In order to avoid such a situation it was decided to design the present samples with the calibrated part machined out of a plate of a much larger thickness, as shown in Fig. 3. The two massive heads thus defined on both sides of the part to be sheared can then be gripped firmly with no damage to the centre of the specimen. These specimens may be machined out of material obtained from extruded plates- or injection-moulded pads. In both cases, an adequate heat treatment might be applied to relax any internal stresses.

2.3. Shear testing machine

The testing apparatus that is described below was designed in order to apply the shearing forces to the specimen by means of a standard tensile machine. The main variables recorded during the test were the shearing force and the shearing displacement. In addition, with a view of obtaining information on the nature of the stress tensor associated with the simple shear deformation, the mean force experienced by the specimen normal to the shearing plane was also measured.

The general features of the machine are illustrated schematically in Fig. 4. Three main parts can be distinguished.

1. The longitudinal slider (LS), to which one of the heads of the sample is attached, is connected to the force transducer of the tensile testing machine.

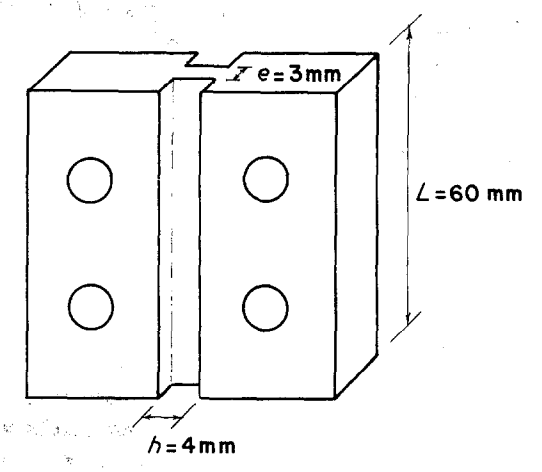

Figure 3 Geometry and dimensions of the specimens.

2. The holding frame (HF) ensures the rigidity of the machine. Its longitudinal movement with respect to the above slider defines the shear straining. It holds the guiding rails and the normal force transducer (NFT), and it is connected to the actuator (A) of the hydraulic tensile testing machine.

3. The transverse slider (TS) is an original characteristic of the present apparatus. It is

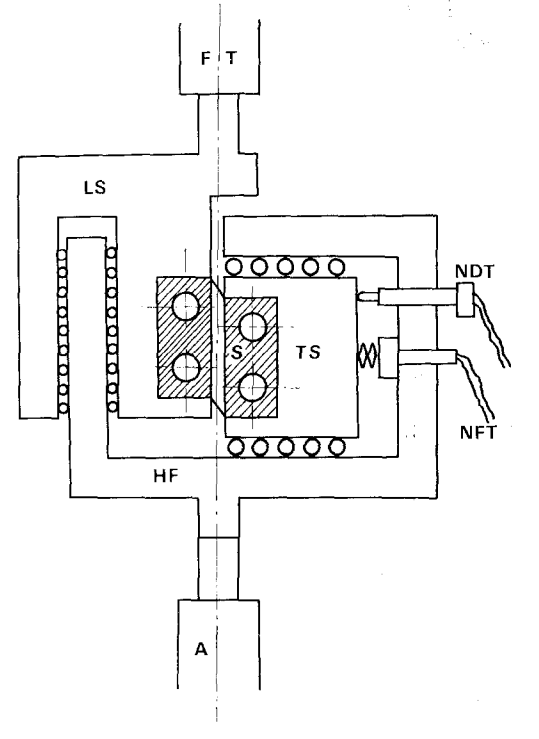

Figure 4 Schematic diagram of the shearing device.

attached to the other head of the sample and provides, if desired, a second degree of freedom perpendicular to the shearing direction. In the course of the tests, since the width h of the specimen was to be kept constant, the slider was firmly attached to the normal force transducer (NFT). However, the transverse slider was allowed to move freely during mounting and gripping, so that no unwanted stresses could be introduced in the calibrated part due to head tightening.

The drawing in Fig. 5 gives a detailed view of the mechanical parts of the shear testing machine. The holding frame and the sliders have been designed to be quite stiff up to a force of the order of 50 kN. On the other hand, the transverse slider must be able to move, particularly at the maximum load, with only a small frictional resistance, corresponding to a friction coefficient of about 3/1000. This is achieved by mounting the sliders on high precision bearings with cylindrical rollers (Schneeberger HW 20). With such bearings, the movement could be kept very smooth with a minimum play. Since the width h of the samples is rather small (4 mm), a good precision in the determination of the strain $\gamma = x/h$ can be obtained only if the relative displacement x of the heads can be imparted and measured with a similar precision. In view of this requirement, particular attention was paid to the heads gripping the specimen. As shown in Fig. 3, both heads have two holes drilled precisely at a distance of 17 mm from the median axis of the calibrated part. The specimens could therefore be tightened between striated steel plates by a set of four bolts passing through these holes. In order to eliminate the error due to the flexure of the bolts produced due to the shearing displacement, two blocking screws are adjusted before the test (labeled BS in Fig. 5). As will be demonstrated later, this special device enabled exact monitoring of the applied shear strain.

Another interesting feature of the present machine is the special fixture attached to the transverse slider. It consists of a kind of piston whose screwed stem connects it to the holding frame. The piston is inserted in a cylindrical cage within the transverse slider. As was pointed out before, the piston may be totally free or blocked in the cage, for installing the specimen

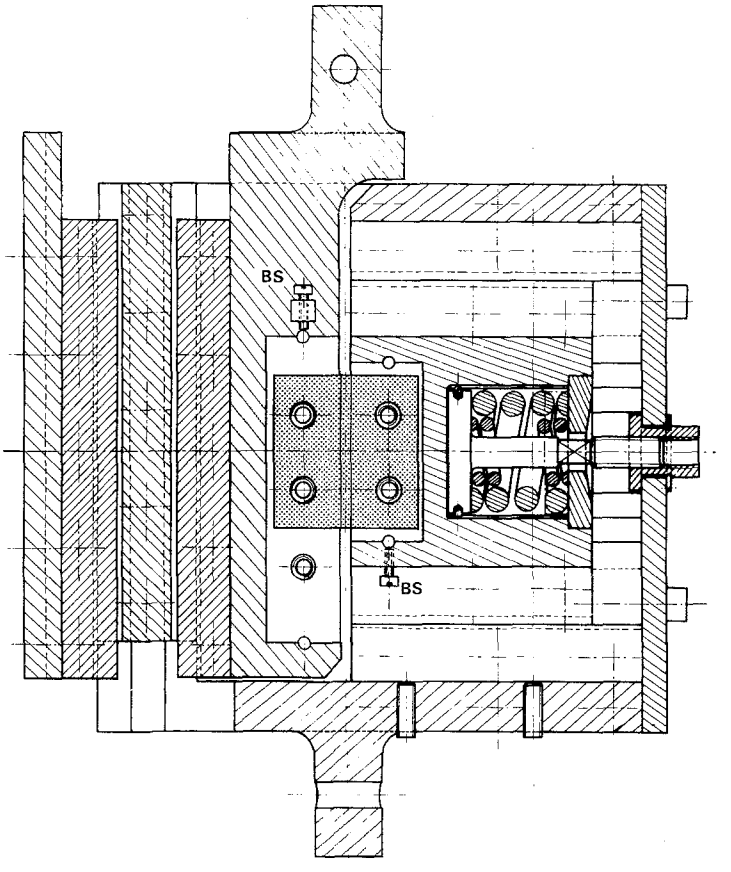

Figure 5 Detailed drawing of the machine.

TABLE I

Material	Abbreviation	Trade mark	Compound reference	Density
High density polyethylene	HDPE	BASF	Lupolen 52612	0.95
Poly propylene	PP	HOECHST	Hostalen PPH 1050	0.90
Polyamide 6-6	PA66	BASF	Ultramid A5	1.13
Poly methylene oxide	POM	DUPONT	Decrin 150	1.41
Polybutene -1	PB1	HULS	Vestolen BT 8000	0.914
Polycarbonate	PC	BAYER	Makrolon L	1.2
Polyvinyl chloride	PVC	–	–	1.38
Polymethyl methacrylate	PMMA	–	–	1.2

or performing standard simple shear tests (constant h). However, by inserting a set of helical springs between the piston and the cage end (Fig. 5) it is also possible to perform tests under constant normal stress (whether tensile or compressive). This option was not extensively used during the present investigation, but could be worthwhile for determining the critical yield stress of materials in biaxial state of stress. In such a case, it may be useful to monitor the variation in the sheared width of the sample; this can be achieved by the normal displacement transducer (NDT) installed between the holding frame and the transverse slider.

This shearing apparatus was mounted on an MTS closed-loop hydraulic testing machine equipped with an environmental chamber for testing under controlled temperature. Simple shear tests could then be performed at shear strain rates $\dot{\gamma}$ between 10^{-1} to 10^{-5} sec^{-1}, and at temperatures between -100 to 200° C. Using proper calibration of the electronic recording table, to which the transducers (displacement, load and mean normal force) were connected, it was possible to display directly the results of the tests as shear stress against shear strain, and mean normal stress against shear strain curves.

2.4 Tested materials

All the specimens tested in the course of this study were machined out of commercially available extruded plates of 10 mm thickness. Their reference and densities are given in Table I. The first five of them are highly crystalline (HDPE, PP, PA66, POM and PB1), while the last three, can be considered as glassy amorphous polymers. Only HDPE was tested for a wide range of experimental conditions (strain rate and temperature). The other materials were tested mainly with the view of determining suitability of the testing method.

3. Experimental results

3.1. Feasibility of the simple shear test

The stress–strain curves displayed in Fig. 6 for the eight tested polymers show that the simple shear testing technique can be applied to ductile polymers as well as to brittle ones. It can be seen that in the

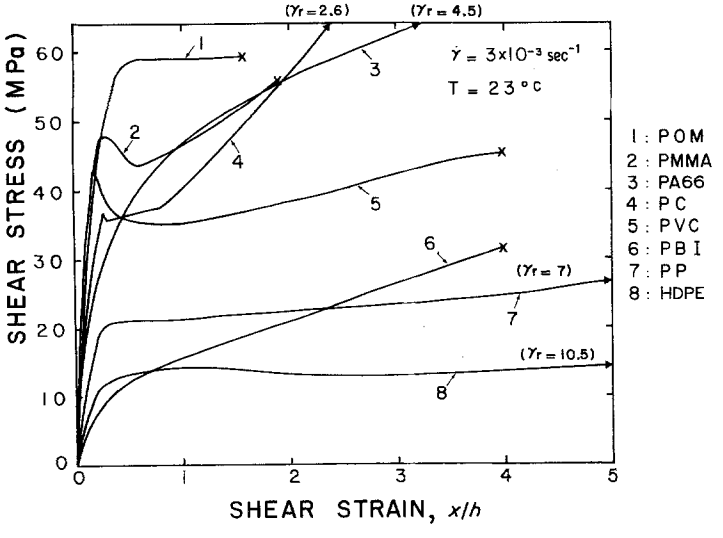

Figure 6 Typical shear stress–shear strain curves obtained with different polymers.

case of polymethyl methacrylate, for instance, rupture occurs at a shear strain as large as 200%, while in tension the same material breaks at room temperature after being strained by only a few per cent. As shown before in torsion experiments [9–10], the simple shear loading is well suited for studying the plasticity of polymeric materials which usually develop early crazing in tension. This is because the critical conditions for craze opening are not fulfilled in simple shear, as demonstrated before in the literature [25]. In the case of usually ductile materials (such as HDPE), the shear test can be conducted up to strains larger than 1000%.

The yield behaviour in simple shear is different for glassy amorphous and for semi-crystalline polymers. For the first category (PMMA, PC and PVC), the transition between the viscoelastic stage and the plastic stage is marked by a stress drop whose magnitude is more pronounced in some cases than others, but which is always very abrupt. In the case of crystalline polymers (POM, PA66, PB1, PP and HDPE), the yield behaviour is more gradual and the viscoelastic to plastic transition appears as a rounded off knee on the curve. However, some of these polymers (PP and HDPE) do show a small stress drop at the beginning of the plastic stage, but as will be shown later, this transient behaviour is extended over a much larger strain range than that for glassy polymers.

The strain hardening in simple shear appears to be smaller for semi-crystalline than for glassy polymers. In both cases, however, it does not increase very much with strain in contrast to the large increase of strain-hardening observed in tension test when the plastic behaviour is displayed in terms of true stress: true strain curve at constant true strain rate (G'Sell and Jonas [3], Hope *et al.* [4]). This point which will be discussed later, can also explain the very large strains experienced by these materials in simple shear.

Specimen rupture occurs in different modes according to the material. Two typical examples are given in Fig. 7 with the photographs of PMMA and HDPE specimens deformed up to rupture. In the first case, fracture occurred in a very brittle way by the initiation and propagation of the oblique sharp cracks from the exterior corners at the specimen ends. In the second case, after a much larger plastic deformation, a fibrillar crack propagated slowly near the heads of the sample,

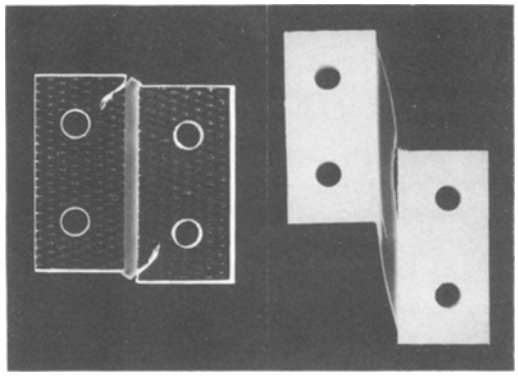

Figure 7 Photographs of tested samples of PMMA and HDPE showing the different rupture types of these two materials.

starting from the interior corner at the specimen ends.

It appears then that the extension of simple shear tests to ultra large strains is limited by end effects which favour the development of tensile stresses causing the cracks. With regard of this limitation the torsion test should prove superior, since the shearing is axisymmetric. However, as shown in previous studies [9, 26], this advantage is only an apparent one since plastic instability soon occurs, so that the final attainable strain is not larger than in the present technique.

3.2. Detailed stress–strain behaviour of high density polyethylene in simple shear

Much attention was paid in this study to the plastic shear behaviour of HDPE, which was investigated previously in uniaxial tension by one of the authors (G'Sell and Jonas [3], G'Sell *et al.* [6]).

The upper curve of Fig. 8 shows the complete shear stress against shear strain curve of HDPE obtained at room temperature for a slow strain rate $d\gamma/dt = 3 \times 10^{-3}\ sec^{-1}$. The curve can be broken up into five stages.

1. Stage I corresponds to the initial viscoelastic response of the material. Unloading the sample in this stage makes the strain revert to zero with a delay of the same order as the loading time.

2. Stage II beginning at $\gamma = 0.3$, is marked by a sudden decrease in the slope of the curve. As shown in Fig. 9, the amount of short term recoverable deformation begins to be reduced abruptly

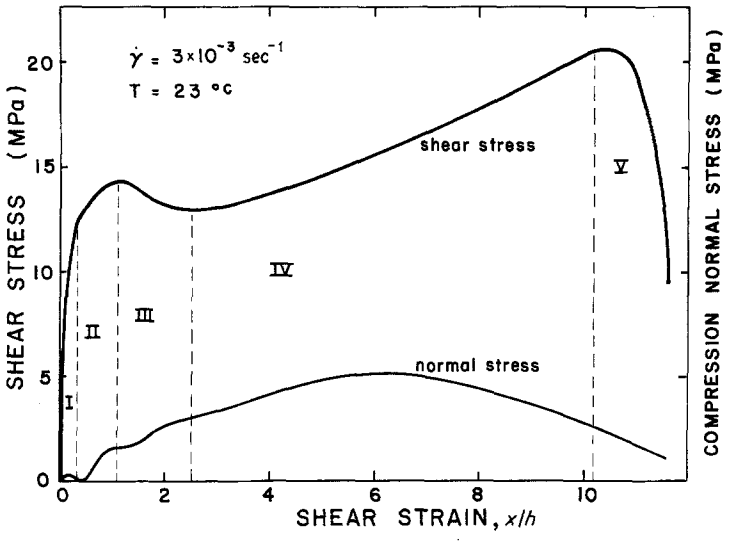

Figure 8 Successive stages of deformation shown by the complete shear stress against shear strain curve for HDPE. Also evolution of the normal compressive stress during a shear test.

within this stage; it can, therefore, be defined as the onset of plastic response. The slope decreases gradually until a maximum stress $\tau_{max} = 14.3$ MPa is reached at about $\gamma = 1$.

3. Stage III corresponds to a stress drop of very small amplitude ($\tau_{max} - \tau_{min} = 1.3$ MPa), spread over a strain range from 1 to 2.6. A careful analysis of the geometric and thermal evolution of the specimen has shown that this stress drop cannot be attributed to a reduction of the sample cross-section (as in the case of necking in tensile testing [3]) nor can it arise from an adiabatic self-heating of the material. (Local measurements in a small cavity drilled at the level of the sheared portion showed that the temperature increase was as small as 1° C.) Its origin has been discussed on the basis of a microstructural model involving crystallite rotation by Boni [27].

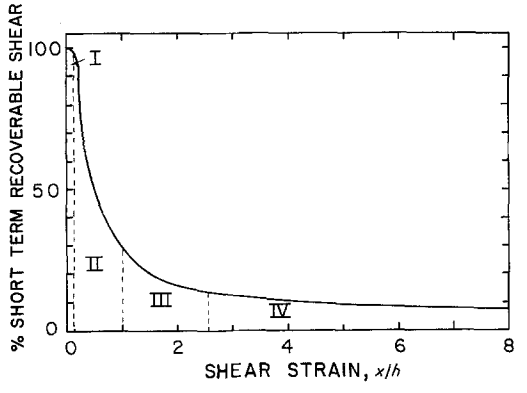

Figure 9 Percentage of short term recoverable strain measured by unloading sequences during a simple shear test with HDPE.

4. Stage IV covers a very large range of shear strain, from $\gamma = 2.6$ to $\gamma \simeq 10$. It is mainly due to plastic deformations and one can note that the strain hardening rate is quite moderate since it is only equal to 1.3 MPa at the end of the stage.

5. Stage V is associated with the gradual development of cracks along the boundary of the heads. As discussed before, rupture begins at the specimen ends and then, due to the inclination of the tensile principal stress, propagates by a succession of steps.

The lower curve in Fig. 8 displays the variation of the mean normal stress measured during the test perpendicular to the direction of simple shear by the normal force transducer attached to the transverse slider of the machine. The normal stress is compressive. It exhibits a wavy variation during stages I, II and III and then increases slowly during stage IV until it reaches 35% of the applied shear stress. For strains larger than 6.4, the normal stress decreases gradually. It can be noted at this point that if the shear test were performed with no normal constraint on the specimen heads (transverse slider being free), the specimen width would increase (up to about 38% of its original value), with a corresponding reduction in the thickness so that the volume would remain essentially constant.

3.3. Homogeneity of the shear strain

Several tests were performed with polyethylene samples which were previously printed with a square array of small dots on the calibrated portion. Photographs were taken sequentially during the tests so that the evolution of local

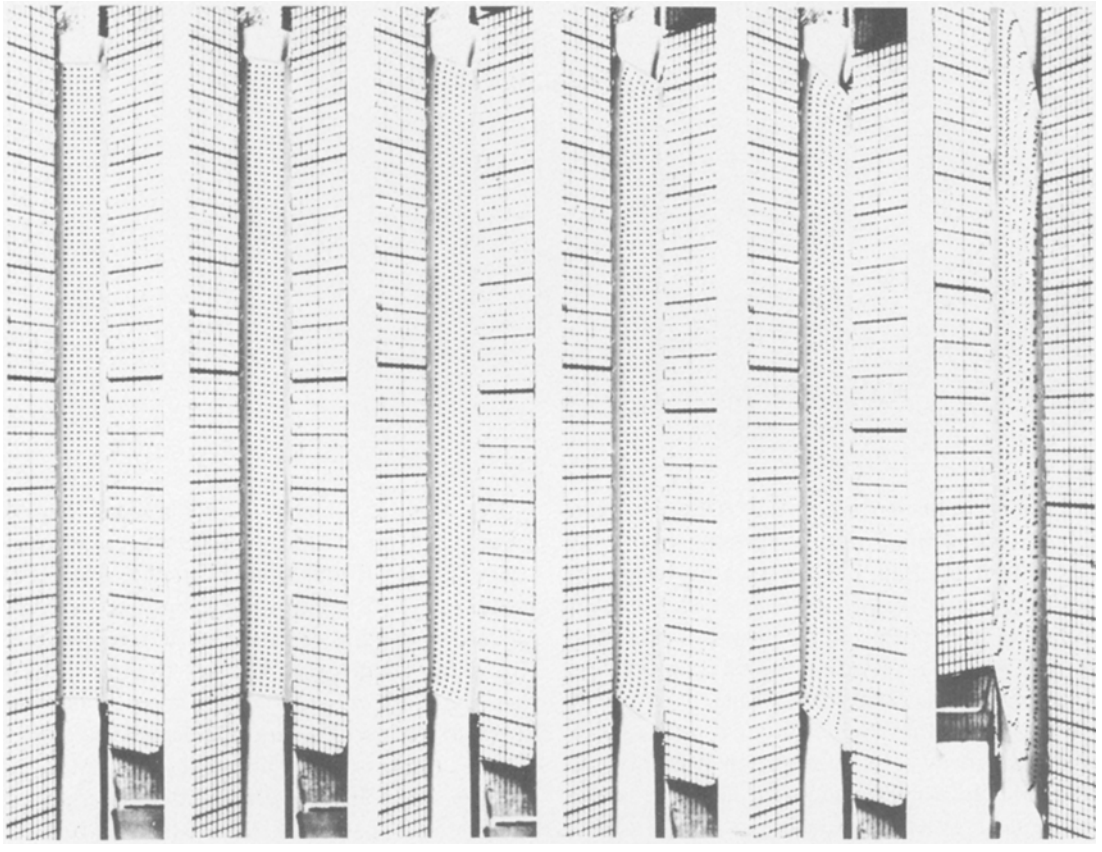

Figure 10 Distortion during a simple shear test of a square array of small dots printed on the specimen surface and observed *in situ* under stress at different values of the shear strain.

shear deformation could be followed without hindering the material response (Fig. 10). Photographs obtained up to $\gamma = 1$ show that the deformation is nearly homogeneous, except in the end regions where the rows of dots are seen to split as in a fan; local compressive strains are induced near one head and local tensile strains near the other head of an end region. (This situation at the ends is closely related to the distribution of constraint stresses depicted in Fig. 2b.) It is seen, however, that the local inhomogeneity at the ends spread only over a distance of the order of the specimen width, $h = 4$ mm. As observed in Fig. 10d, the sheared array of dots at $\gamma = 1$ exhibits again a square-like symmetry. This demonstrates that the applied shear strain is uniform to a very good precision, thanks to the special screws which block the movement of the sample heads prior to the test initiation.

The photographs obtained at larger strains are more difficult to analyse because some of the adhesive dots tend to be torn. It is found, however, that stage III of the stress against strain curve (stress drop) is associated with a development of a strain inhomogeneity; a vaguely defined shear band develops in the median part of the specimen where the local shear is larger by about 1 than the mean applied shear. A detailed investigation presented by Boni [27] shows that this plastic instability heals gradually at larger strains so that the deformation retrieves its original homogeneity at $\gamma \simeq 5$.

3.4. Influence of strain rate and temperature

The shear stress against shear strain curves displayed in Fig. 11 were obtained with uniform shear strain rates, $\dot{\gamma} = d\gamma/dt$, ranging from 3×10^{-5} to 5×10^{-1} sec^{-1}. One notes at once that the curves at the fastest strain rates diverge from

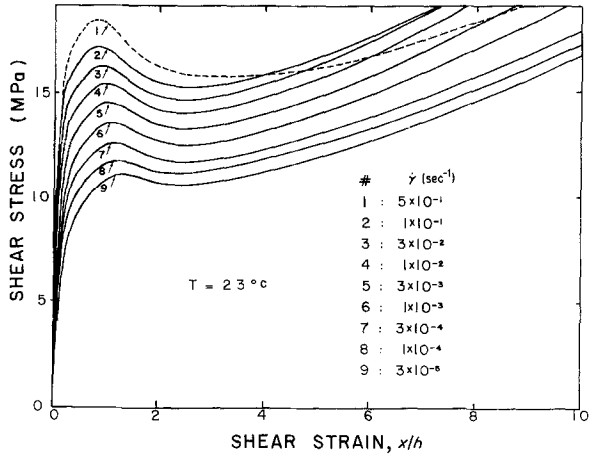

Figure 11 Influence of the strain rate on the simple shear behaviour of polyethylene.

the general tendency that the stress increases with increasing strain rate. In agreement with the investigation by Hall [28] on tensile tests, this observation is explained by the noticeable self-heating which appears at strain rates faster than 3×10^{-2} sec^{-1}. A simple thermal computation shows indeed that the heat dissipated by plastic deformation within the calibrated part can be eliminated mainly by conduction towards the heads of the samples and that a rather sharp transition is observed around $\dot{\gamma} = 3 \times 10^{-2}$ sec^{-1} from the isothermal to adiabatic region.

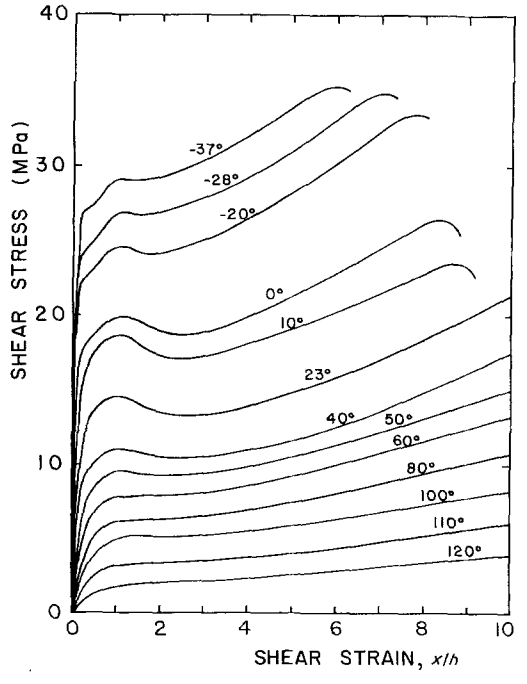

Figure 12 Influence of temperature on the simple shear behaviour of polyethylene.

For slow strain rates it is observed that the influence of the strain rate is different in the yield region (stages II and III) and in the long plastic region (stage IV). The stress drop is considerably reduced in magnitude as the strain rate decreases. (By extrapolating the data, it can be deduced that the drop would be suppressed completely at about 10^{-7} sec^{-1}, which indicates its transient nature.) Conversely, in the steady-state, stage IV, the stress is gradually lowered with decreasing rate, but the strain-hardening stays equal, so that one curve could be obtained from another by a vertical shift.

All the curves in Fig. 12 were obtained at the same strain rate (3×10^{-3} sec^{-1}), at temperatures from -37 to 120° C. It is seen that the yield drop is suppressed completely at temperatures approaching the melting point. At low temperatures, the drop is also attenuated, but this is due both to the rise of stage II critical stress and to the increase in the strain-hardening of stage IV. Lastly, one can note that the ultimate strain at rupture is decreased drastically at low temperatures since the stress concentrations at sample ends cannot be relaxed very easily.

From such a set of curves, a constitutive equation can be derived to describe the plastic behaviour. Such an analysis has been presented previously by Boni [27].

4. Discussion

4.1. Kinematics of simple shear deformation

Consider a rectangular parallelepipedic body whose material points in the undeformed state are specified by the Cartesian coordinates X_1, X_2 and X_3 parallel to its three edges. A deformation of the

solid in simple shear is described by

$$x_1 = X_1 + \gamma(t) X_2$$
$$x_2 = X_2$$
$$x_3 = X_3 \qquad (5)$$

where x_1, x_2 and x_3 are the Cartesian coordinates of the material points after deformation. Since x_i are linear functions of X_i, the deformation is homogeneous. A circle of radius 1 drawn on the $X_1 - X_2$ face (i.e. $X_1^2 + X_2^2 = 1$) deforms into an ellipse [29]

$$x_1^2 - 2\gamma x_1 x_2 + x_2^2 (\gamma^2 + 1) = 1. \qquad (6)$$

The orientations of the major and the minor axes of this ellipse are as shown in Fig. 13. As discussed below, these axes define the principal axes of strain in their current position. The angle α which the major axis of the ellipse makes with the Ox_1 axis, can be shown to be equal to $\frac{1}{2}\tan^{-1}(2/\gamma)$. Thus, in contrast to the small strain theory (for which $\gamma \ll 1$ and $\alpha = 45°$), it is seen that $\alpha < 45°$ and decreases progressively with the deformation. The above geometric interpretation can be shown equivalent to the following analytic definition of finite strain:

$$2\eta_{ij} = \delta_{ij} - \sum_{k=1}^{3} \frac{\partial X_k}{\partial x_i} \frac{\partial X_k}{\partial x_j} \qquad (7)$$

where δ_{ij} is the Kronecker delta and η_{ij} are the Cartesian components of the Eulerian finite strain tensor [30]. Using Equations 5 and 7 it follows that in the case of simple shear this tensor is

$$[\eta] = \eta_{ij} = \begin{bmatrix} 0 & \gamma/2 & 0 \\ \gamma/2 & -\gamma^2/2 & 0 \\ 0 & 0 & 0 \end{bmatrix}. \qquad (8)$$

Now, from the Mohr's circle construction, it can be verified that the principal strains η_1 and η_2 have the same direction as the major and minor axes of the strain ellipse (Equation 6) and that the value of a principal strain is related to the length of the axis with which it coincides. Thus there is a complete correspondence between the analytical definition Equation 8 and the graphical representation, Fig. 13.

Another kinematic quantity of importance is the rate of deformation tensor, which is a measure of the immediate change of configuration

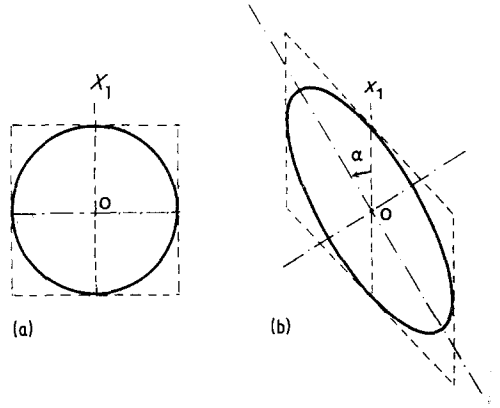

Figure 13 Distortion of a circle under simple shear and geometrical definition of the principal axes of strain.

with respect to the current configuration of the body. It is defined as

$$2D_{ij} = \left[\frac{\partial v_i}{\partial x_j} + \frac{\partial v_j}{\partial x_i}\right] \qquad (9)$$

where v_i the i^{th} velocity component of a material point. For the simple shear deformation this tensor is

$$[D] = D_{ij} = \begin{bmatrix} 0 & \dot{\gamma}/2 & 0 \\ \dot{\gamma}/2 & 0 & 0 \\ 0 & 0 & 0 \end{bmatrix} \qquad (10)$$

where $\dot{\gamma}$ is the shear rate. Here, in contrast to the total components, we note that the rate components maintain their principal values at 45° regardless of how large the shear (γ) is. These two tensors will be used in the following discussion of the constitutive equations.

4.2. Relation of stress tensor to deformation

As a simple example of constitutive equations, we first consider the simple shear deformation of an isotropic rigid-plastic body (exhibiting no elasticity) and obeying the von Mises yield condition. The constitutive equations for such a material are given by the Mises flow rule, i.e.

$$\sigma_{ij} - p\,\delta_{ij} = fD_{ij} \qquad (11)$$

where σ_{ij} is the component of the *true* stress tensor, $p = (\sigma_{11} + \sigma_{22} + \sigma_{33})/3$ is the "hydrostatic" part of the stress and f is a function expressing the hardening characteristic of the material. Equation 11 states that the material response is such that the principal axes of stress tensor $[\sigma]$

coincide with the principal axes of deformation rate tensor $[D]$. This condition of the coincidence of the two sets of principal axes signifies isotropic behaviour. Since the principal axes of $[D]$ in the simple shear deformation remain at 45° with respect to the coordinate axes, so do the principal axes of $[\sigma]$. Also since no traction is applied at the faces x_3 = constant, one has $p = 0$ and thus, the only stresses present are the shear stresses $\sigma_{12} = \sigma_{21} = f\dot{\gamma}/2$. In other words, no normal stresses are induced regardless of how large shear (γ) is. Fig. 14a shows the Mohr's circle for this state of stress.

We consider next the constitutive equations for an isotropic elastic solid. The concept of elasticity is usually taken to mean that the stress is dependent only on the strain measured from a natural, stress-free state and not on the strain rate or strain path. Based on these assumptions, it can be shown that the principal axes of stress tensor $[\sigma]$ are coincident with the principal axes of strain tensor $[\eta]$. Taking into account the resulting rotation of the principal axes, the state of stress is then represented by the Mohr's circle in Fig. 14b for the case of simple shear. It is seen that due to the finiteness of strain, not only the shear stress σ_{12} but also the normal stress, σ_{11}, σ_{22} and σ_{33} are required to produce the shear deformation. (For infinitesimal γ, the normal stresses should, of course, be negligible.) The presence of the normal stress is known as the Kelvin effect [30]. Since the angle β in the Mohr's circle in Fig. 14b is given by $\beta = \frac{1}{2}\tan^{-1}(2/\gamma)$, the normal stresses are then related to the shear stress by

$$\sigma_{12} = (\sigma_{11} - \sigma_{22})/\gamma. \qquad (12)$$

Equation 12 holds independent of the material response functions and thus, is a consequence solely of the assumption of isotropic, elastic material behaviour. It is, therefore, called a universal relation. In addition, since $\sigma_{12}\gamma$ is always positive, it follows that $\sigma_{11} - \sigma_{22} > 0$. This inequality of the normal stresses is known as the Poynting effect [30]. If the material is compressible, then, since simple shear is a volume preserving deformation, the hydrostatic part of the stress must be zero, i.e. $\sigma_{11} + \sigma_{22} + \sigma_{33} = 0$. In this case, the stress σ_{33} is non-zero and is determined by the material response. It must be applied to maintain the state of plane simple shear, and failure to do so will result in some change of dimension in the x_3 direction. However, on the basis of experimental observations, it is reasonable to postulate that for nearly incompressible materials, such thickness changes are negligible, and σ_{33}, if allowed to develop, would remain small. This assumption then leads to $\sigma_{11} \approx -\sigma_{22} \approx \sigma_{12}\gamma/2$.

If one considers now the case when the material undergoes both the finite elastic and the finite plastic deformations, the situation is far from clear, and is a subject of current controversy [31, 32]. According to Lee and McMeeking [32], if the strains are finite, then in general $d\epsilon_{ij}$ (elastic) $\neq d\epsilon_{ij}$ (recoverable) and, $d\epsilon_{ij}$ (plastic) $\neq d\epsilon_{ij}$ (residual). In other words, there is a coupling effect between the elastic and plastic strains, and the elastic increment of strain is not fully recovered when the increment of stress is removed. However, if the elastic strains are small (as for example, in the case of metals), or if the deformation is such that the principal axes of strain do not rotate (for example in a tension test), then such effects are either negligible or absent. In view of the unsettled state of the above matter, and relatively small elastic strains, we assume in analogy with the tension test, that $\gamma = \gamma_{\text{elastic}} + \gamma_{\text{plastic}}$, where γ_{elastic} is the short term recoverable strain shown in Fig. 9 for a typical test on polyethylene samples. The normal stress effect may be considered solely due to this component of strain. Then as discussed above, the normal stress σ_{22} monitored during the test should vary according to the relation $|\sigma_{22}| = (\frac{1}{2})\tau\gamma_{\text{elastic}}$, where τ is the applied shear stress. Fig. 15 shows that the experimentally measured normal stress is indeed of the same order of magnitude as the predicted one, up to $\gamma \simeq 6$. For very large strains, however, one observes a drop in the normal stress. This drop can be due to the development of an anisotropic fibrous texture in the highly deformed polymer sample.

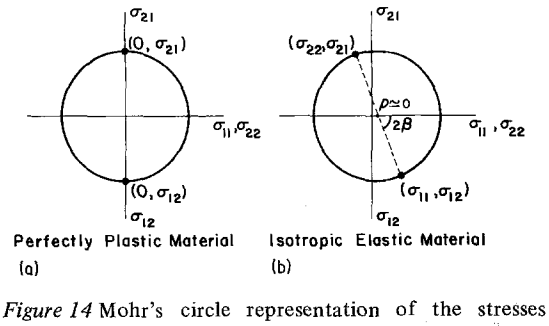

Figure 14 Mohr's circle representation of the stresses under simple shear: (a) for a perfectly plastic material, and (b) for an isotropic elastic material.

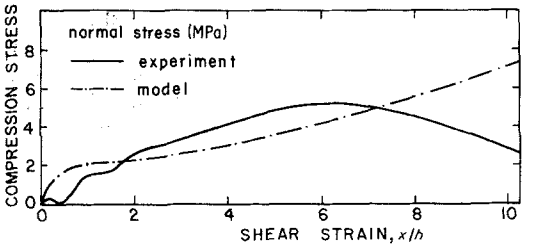

Figure 15 Comparison of the normal compressive stress recorded experimentally and predicted by the model.

In conclusion, it may be stated that for the materials presently tested, the applied shear stress τ, as measured in the simple shear tests, is fairly close to the true shear stress, and can be used for expressing the true shear stress–true shear strain behaviour of these materials in the plastic range. That the normal stresses cause no major perturbation of the state of pure shear stresses ($\sigma_{12} = \sigma_{21} = \tau$, other $\sigma_{ij} \simeq 0$), is seen by noting that $\tau_{max} = \tau[1 + (\sigma_{22}/\tau)^2]^{1/2}$, from the Mohr's circle Fig. 14b, is larger than τ by at most 6%, when the normal stress is maximum.

4.3. End effects

The observation of the deformation by means of a grid of dots, (Fig. 10) has proved that the ends of the specimens were affected by strain inhomogeneity. This perturbation had two apsects: 1. the lines of dots normally parallel to the shear direction were either compressed against one head, or pulled aside near the other head, and 2. the free side of the sample was curved and had a convex (bulging) curvature. These observations are explained on one hand by the constraint effect of the grips, which react against the rotational moment imposed by the couple of the shearing forces, and on the other hand by the deparature from the ideal simple shear condition in which the ends of the specimen must also carry appropriate tractions, in general normal to and parallel to the end surfaces.

In order to check the general validity of these observations, the stresses, strains and displacements in a model specimen were calculated by the finite element method with the NONSAP program developed at the University of California by Bathe *et al.* [33]. True to the experimental condition, the transverse end surfaces in the finite element model were considered to be traction free, and the longitudinal surfaces were given a relative shear displacement. The material was taken to be isotropic elastic, with a Mooney–Rivlin strain energy function [30]. With such an elastic behaviour, the components of the stress tensor under simple shear can be shown to be $\sigma_{11} = 2C_1\gamma^2$, $\sigma_{22} = -2C_2\gamma^2$ and $\sigma_{12} = 2(C_1 + C_2)\gamma$. In order to simulate the zero hydrostatic hydropressure postulated above, a unique value of 10 MPa was assigned to both constants C_1 and C_2. The specimen size, for the demonstration purpose, was chosen as shown in Fig. 16a, and was divided into several small rectangular elements. Fig. 16b shows the deformed geometry of the specimen and its elements at $\gamma = 1$. We note that essentially all the features of the end effects detected experimentally are reproduced by the finite element calculations. In particular, the presence of the tensile and compressive strains which affect the zones near both heads is apparent by the curvature of the lines parallel to the X_1 axis.

In considering the application of the present testing technique, the occurrence of the zones of localized transverse tensile stresses at the specimen ends is worrisome, because it leads to the development of flaws during the testing. This problem was encountered when the present technique was applied to the simple shear testing of carbon fibre-reinforced polymers. It was found that the measured interlaminar shear strength was exceedingly low, due to the preferential opening of cracks along the fibres at the specimen ends. In agreement with the previous conclusions of Whitney [34], it was shown that a correct value of the shear strength of the composite materials was obtained by orienting the specimen so that the fibres are perpendicular to the shear direction. Fortunately, in the present case of thermoplastic polymers, this problem of local embrittlement at the specimen ends becomes critical only at large strains. Furthermore, the perturbation to the strain distribution caused by the end effect is shown by Fig. 16 to be significant only in end zones of length equal to the width of the sample. Hence, because of their large length to width ratio, the overall perturbation is negligible in the present specimens.

4.4. Comparison of the plastic behaviour in simple shear and in uniaxial tension

It has been noted in a previous section, that the strain hardening capability of the polymers tested in simple shear was found to be rather weak. In order to compare the present results with those obtained in the tensile tests, the stress–strain

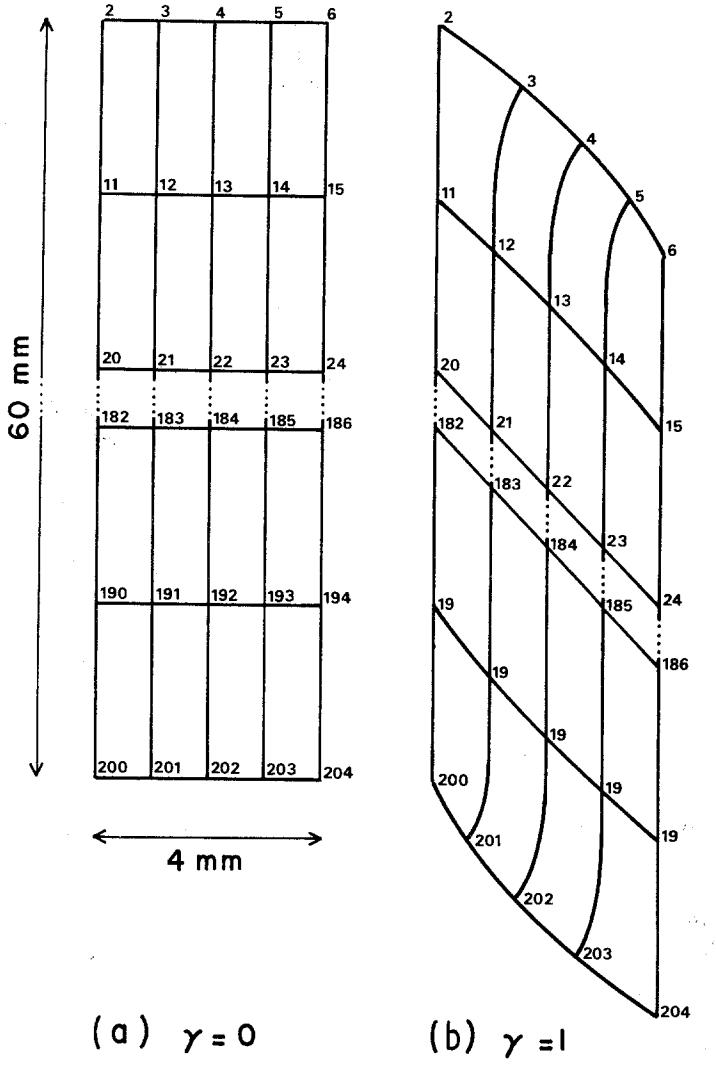

Figure 16 Finite element prediction of the end effects during the simple shear of Mooney–Rivlin elastic material: (a) undeformed grid, and (b) deformed grid at $\gamma = 1$.

data obtained from both types of tests must be converted into the equivalent stress–equivalent plastic strain curves. If the material obeys the von Mises yield criterion and if the progressive strain hardening does not induce any anisotropy, then the equivalent stress–equivalent plastic curves should be the same for the two types of test, or, in fact, for any general (multiaxial) deformation path.

The von Mises equivalent stress in simple shear is given by

$$\sigma_{eq} \approx [3(\tau^2 + \sigma_N^2)^{1/2}] \approx 3^{1/2}\tau \qquad (13)$$

where $\tau = \sigma_{12}$ and $\sigma_N = |\sigma_{22}| \approx \sigma_{11}$ under the assumptions discussed above.

The calculation of the equivalent plastic strain is not straight forward, and has been presented for the case of simple shear by Canova *et al.* [35]. It is obtained by integrating its increment $d\epsilon_{eq}$ along the deformation path. Actually, the increments refer to the plastic strain only. Ignoring this restriction which is relevant only at small strains, the equivalent strain is given by

$$\epsilon_{eq} = \gamma/(3^{1/2}). \qquad (14)$$

From the definitions and Equations 13 and 14, the equivalent stress–equivalent strain curve was obtained for the simple shear test on the polyethylene sample performed at the strain rate $\dot{\gamma} = 3 \times 10^{-3}\ \text{sec}^{-1}$. The corresponding curve for the tension test was obtained at $\dot{\epsilon}_{11} = 1.7 \times 10^{-3}$ sec^{-1}, using the technique described by G'Sell and Jonas [3] which gives the true stress–true strain curve at constant true strain rate. These curves are shown in Fig. 17. It may noted that the specimens for both types of tests were machined from the

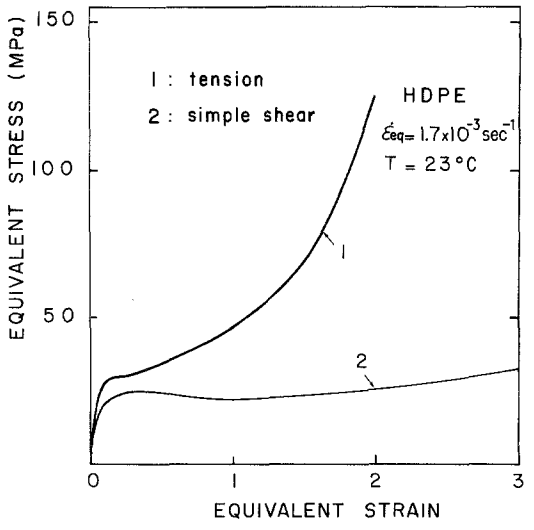

Figure 17 Comparison of the plastic behaviour of polyethylene under uniaxial tension and simple shear.

sample plate. By comparising the two curves, it can be seen that 1. the equivalent yield stress is very close in tension and in simple shear, as found previously from torsion tests at small strains [36] (the difference of about 15% between the equivalent yield stresses in uniaxial tension and in simple shear can be due to experimental errors and also to the limited adequacy of the von Mises criterion to represent the critical yielding conditions) and 2. the strain hardening in tension is far larger than in simple shear.

The interpretation of the noticeable difference between the curves at large strain is now under investigation. At this stage of the study, it is postulated that it could be due to the development of different microscopic textures in specimens deforming under the two states of strain, as proposed earlier for metals by Gil-Sevillano and Aernoudt [37]. It appears here that whereas simple shear favours the glide of macromolecular chain along a unique plane, tensile drawing initiates glide on an infinitude of intersecting planes included to the tensile axis, leading to the formation of chain tangles which increase the resistance to further plastic flow.

5. Summary and conclusions

Plane simple shear tests were performed at constant shear strain rate on various thermoplastic polymers by means of a new type of shearing apparatus. It was shown that a nearly homogeneous plastic shear strain could be achieved without buckling, provided the thickness, width and length of the sample's calibrated part are proportional to 3, 4 and 60, respectively. Due to the absence of crazing, large shear strains could be reached before rupture, even for polymers which exhibit a very brittle behaviour in tension, e.g. PMMA. In the particular case of HDPE, the plastic behaviour (γ, $\dot{\gamma}$, τ) was determined from a series of tests at different strain rates and temperatures. It was found that the shear stress is highly dependent on temperature while the strain rate sensitivity is rather small. Also the strain hardening under simple shear was found to be very small, in comparison with the uniaxial tensile behaviour (compared on the basis of equivalent stress and strain). It appears then that the simple shear test, if conducted with proper sample size and machine strength, gives reliable stress–strain data which can be used in conjunction with tensile test data to predict plastic behaviour of polymers under more complex state of strain and stress.

Acknowledgements

The authors are indebted to the French Delegation Generale à la Recherche Scientifique et Technique for financial support (Contract No. 79.7.0931). They are grateful to the Ministère des Relations Extérieures (France) and to the Ministère des Affaires Intergouvernementales (Quebec) for the award of a France–Quebec Research Fellowship.

References

1. C. A. PAMPILLO and L. A. DAVIS, *J. Appl. Phys.* **43** (1972) 4277.
2. S. BAHADUR, *Polym. Eng. Sci.* **13** (1973) 266.
3. C. G'SELL and J. J. JONAS, *J. Mater. Sci.* **14** (1979) 583.
4. P. S. HOPE, I. M. WARD and A. G. GIBSON, *ibid.* **15** (1980) 2207.
5. N. J. MILLS, *Brit. Polym. J.* **10** (1978) 1.
6. C. G'SELL, A. ALY-HELAL and J. J. JONAS, submitted to *J. Mater. Sci.*
7. J. C. M. LI, *Met. Trans.* **A9** (1978) 1353.
8. A. S. ARGON, R. D. ANDREWS, J. A. GODRICK and W. WHITNEY, *J. Appl. Phys.* **39** (1968) 1899.
9. W. WU and A. P. L. TURNER, *J. Polym. Sci.* **11** (1973) 2199.
10. *Idem, ibid.* **13** (1975) 19.
11. K. D. PAE and A. A. SILANO, *J. Appl. Polym. Sci.* **22** (1978) 3021.
12. P. B. BOWDEN and J. A. JUKES, **3** (1968) 183.
13. K. T. EDWARD, *Fiber Sci. Tech.* **5** (1972) 83.
14. R. E. ROBERTSON, *J. Polym. Sci. (A2)* **7** (1969) 1315.
15. R. E. ROBERTSON and C. W. JOHNSON, *J. Appl. Phys.* **37** (1966) 3969.
16. *Idem, J. Polym. Sci. (A2)* **6** (1968) 1673.

17. N. BROWN and I. M. WARD, *ibid.* **6** (1968) 607.
18. N. BROWN, R. A. DUCKETT and I. M. WARD, *Phil. Mag.* **18** (1968) 483.
19. G. E. DIETER, "Mechanical Metallurgy", (McGraw Hill, New York, 1961) p. 16.
20. S. BONI, C. G'SELL, E. WEYNANT and J. M. HAUDIN, *Polym. Test.* **3** (1982) 3.
21. E. J. HEARN, "Mechanics of Materials" Vol. 1, (Pergamon Press, Oxford, 1977) p. 320.
22. R. V. SOUTHWELL, *Phil. Mag.* **48** (1924) 540.
23. F. BLEICH and H. BLEICH, "Buckling Strength of Metal Structures", (McGraw Hill, New York, 1952).
24. S. P. TIMOSHENKO and J. M. GERE, "Theory of Elastic Stability", (Dunod, Paris, 1966) p. 379.
25. S. S. STERNSTEIN, L. ONGCHIN and L. SILVERMAN, *Appl. Polym. Symp.* 7 (1968) 175.
26. A. A. SILANO, K. D. PAE and J. A. SAUER, *J. Appl. Phys.* **48** (1977) 4076.
27. S. BONI, These d'Ingenieur, CNAM, Nancy (1981).
28. I. H. HALL, *J. Appl. Polym. Sci.* **12** (1968) 731.
29. J. C. JAEGER, "Elasticity, Fracture and Flow", (Chapman and Hall, London, 1959) p. 28.
30. R. J. ATKIN and N. FOX, "An Introduction to the Theory of Elasticity", (Longman, 1980).
31. S. NAMET-NASSER, *Int. J. Solids Struct.* **15** (1979) 155.
32. E. H. LEE and R. M. McMEEKING, *ibid.* **16** (1980) 715.
33. K. J. BATHE, E. L. WILSON and R. H. IDING, Report No. UCSESM 74-3, University of California, Structural Engineering Laboratory, 1974.
34. J. M. WHITNEY, *J. Comp. Mat.* **5** (1971) 24.
35. G. R. CANOVA, S. SHRIVASTAVA, J. J. JONAS and C. G'SELL, "Formability of Metallic Materials – 2000 A.D.", edited by J. Newby and A. Niemeier (ASTM, Philadelphia, 1982) p. 189.
36. P. D. EWING, S. TURNER and J. G. WILLIAMS, *J. Strain Anal.* 7 (1972) 9.
37. J. GIL-SEVILLANO and E. AERNOUDT, *Met. Trans.* **6A** (1975) 2163.

Received 11 February
and accepted 31 August 1982